Size Effect on the Photoluminescence Shift in Wide Band-Gap Material: A Case Study of SiO_2-Nanoparticles

Yit-Tsong Chen[1,2]

[1]*Department of Chemistry*
National Taiwan University
Taipei, Taiwan 106, R.O.C.
[2]*Institute of Atomic and Molecular Sciences*
Academia Sinica, P.O. Box 23-166
Taipei, Taiwan 106, R.O.C.

Abstract

In this article, I will discuss the optical properties of SiO_2-nanoparticles that we have investigated recently by photoluminescence (PL) spectroscopy. In particular, I will show the blue-shifts of PL, originating from the electron-hole recombination of the self-trapped exciton (STE), observed in smaller-sized SiO_2-nanoparticles. To explain the size effect in relating to the STE PL shift, a question has been raised on whether it is appropriate to apply the quantum confinement (QC) theory usually used for the Mott-Wannier type excitons in semiconductors to wide band-gap material, such as silica. In this study, a laser-heating model of free excitons (FEs) to activate lattice phonons has been developed, rather than the QC effect, to interpret the blue-shifts of STE PL in smaller-sized SiO_2-nanoparticles. The blue-shift of STE PL is actually resulted from phonon-assisted PL due to the thermalization of the SiO_2-nanoparticle system during laser irradiation.

***Key Words*:** Size Effect, Photoluminescence, SiO_2 Nanoparticles

1. Introduction

Tremendous amount of research effort has been made recently for the studies of nanometer-sized materials. From industrial point of view, it has always been a dream to reduce the size of electronic devices. Aiming at this goal, a great deal of interest in the research of nanoscale materials has been aroused. The successful development of this nano-research will have dramatic impact on people's daily life. Looking at this nano-study from an academic angle, understanding the chemical, physical, mechanical and optical properties of nanoscale materials is bridging a gap of knowledge between free molecules and bulky materials.

Silica (SiO_2) is a typical wide band-gap insulator (the band-gap of bulk silica $E_g \cong 11$ eV) [1]. Therefore, the bulk SiO_2-based material is characterized by high transparency in ultraviolet spectral range resulting in many important technological applications. The properties of this bulky material have been extensively studied for an appreciable length of time and also been quite well established [1-29]. On the other hand, modern nanoscale technology requires the production of nanometer-sized SiO_2 films and layers, which are of frequent use in silicon-based electronic devices for passivation and electrical insulation. A typical example is the design of combined Si/SiO_2 systems, such as metal-oxide-semiconductor (MOS), nanoscale silicon optoelectronic devices and Si/SiO_2 superlattices [30-34]. The thickness of SiO_2 layers existing in these combined systems usually ranges several nanometers. Since the properties of SiO_2-based nanoscale materials are

somewhat different from those of the bulk, a great body of investigations has recently been devoted to the study of nanoscaled SiO_2-objects (e.g. nanoparticles, nanowires, Si/SiO_2 superlattices etc.) [35-44].

It was generally conceived that photoluminescence (PL) of the combined Si/SiO_2 nanoscale objects are determined by the light-emitters located either inside silicon nanoscales or on the Si/SiO_2 interface [32-34]. Accordingly, quantum confinement (QC) on excitons in variously sized silicon nanoscales has been proposed as a model to explain the visible PL from surface-oxidized silicon nanocrystals [45,46] and porous silicon [47,48]. As a consequence, the nanometer-sized SiO_2 layer covering nanoscale silicon fragments was regarded as only a passivating layer, and presumably counts very little in the PL properties of the nanoscale materials [45-49]. However, from the most recent models concerning the QC effect in silicon nanocrystals and radiative states associated with the Si/SiO_2 interface [34,50], it is evident that the nanometer-sized SiO_2 layer is essential to the PL characteristics of nanoscaled Si/SiO_2 systems. Even though examination of the optical properties of such extremely thin SiO_2 layer presents considerable challenge, experimental study of SiO_2-based nanomaterials by PL spectroscopy is intriguing, and spectral analysis to understand the origins of the observed PL features and their related dynamical mechanisms is far-reaching.

In this article, I will discuss the PL from SiO_2-nanoparticles that we have investigated recently in our laboratory. In particular, I will show the blue-shifts of PL, originating from the electron-hole recombination of the self-trapped exciton (STE), in smaller-sized SiO_2-nanoparticles that we observed by PL spectroscopy. To explain the size effect in relating to the blue-shifts of STE PL, a question has been raised on whether it is appropriate to apply a QC model to wide band-gap material, such as silica. In this study, a laser-heating model of free excitons (FEs) to activate lattice phonons has been developed, rather than the QC effect, to illuminate the blue-shifts of STE PL in smaller-sized SiO_2-nanoparticles. The blue-shift is resulted from the phonon-assisted STE PL in SiO_2-nanoparticles caused by the thermalization of the SiO_2-particle system due to frequent collisions between FEs and nanoscale boundary during laser irradiation.

The rest of this paper is organized as follows. The SiO_2-nanoparticles and experimental set-up for their PL spectroscopic measurements are described in Section 2. Next, results and discussion for the size effect on the STE PL in SiO_2-nanoparticles interpreted with a laser-heating model are presented in Section 3. Finally, conclusions are addressed in Section 4.

2. Experimental

In the PL experiment, two kinds of variously sized SiO_2-nanoparticles (Aerosil, Degussa) in comparison with type-III fused silica as a bulk material were studied. According to the vendor's specification, the commercially available SiO_2-nanoparticles of a specific surface area 300 and 160 m^2/g have the nominal particle sizes of 7 nm and 15 nm (diameter), respectively [44].

PL measurements were performed using an ArF pulsed laser (Lumonics, EX-742; λ_{exc} = 193 mm, duration time = 20 ns, repetition rate = 10 Hz) as an excitation source. The laser beam was focused, particularly for the two-photon excitation experiments, and the intensity could be variably reduced by a set of quartz plates [51,52]. Care was taken to insure that no specimen was damaged during laser irradiation in the applied intensity range. The sample was oriented to the laser beam by 45°, and the PL was collected in conventional 90° geometry by a 0.5 m SpectraPro-500 monochromator (Acton Research Corporation) with 1200 grooves/mm grating blazed at the wavelength of interest. For conventional PL detection, a water-cooled charge-coupled device (CCD) camera (Princeton Instruments; 330×1100 pixels) was employed to monitor the PL signal with an accumulation time of 2 s. For a time delay-gated measurement, the PL was detected by a photomultiplier (Hamamatsu, R943-02; peak wavelength 300–800 nm) and processed through a gated integrator system (Stanford Research System, Model 250). A set of optical filters has been used to cut scattered laser light from the sample. An oscilloscope (LeCroy, Model 9314A) was employed to measure the PL decay time-constants.

3. Results and Discussion

3.1 PL Spectra of SiO_2-Nanoparticles

Figure 1 shows typical PL spectra at 1.5–3.5 eV for 7-nm and 15-nm SiO_2-nanoparticles, respectively, measured at room temperature with

excitation wavelength of 193 nm. Overall, the PL spectra consist of three contributions located in the red (~1.9 eV), green (~2.35 eV), and blue (~2.8 eV) spectral ranges [44,51,52]. The red band peaked at ~1.9 eV results from the non-bridging oxygen (NBO; $Si-O\cdot$) hole centers. The intensity of the NBO band increases dramatically with heat pretreatment of the SiO_2-nanoparticles from 600 to 900 °C, indicating an increase of generating the $Si-O\cdot$ defects in the nanoparticles during the thermal heating [10,13,36,44,51,52].

The green band at ~2.35 eV has been attributed to hydrogen-related species in the composites of SiO_2-nanoparticles [44]. It is well understood that the surface of SiO_2-nanoparticles is quite easily contaminated by water vapor resulting in hydrogen-related chemical bonds, such as Si-H, Si-OH etc. [51]. This surface coating is evidenced in the present observation of the vibrational progression of $\Delta\nu$ = 630 cm^{-1} due to Si-H bending vibration on the surface of 15-nm SiO_2-nanoparticles (lower trace in Figure 1) [44]. The assignment associated with the hydrogen-related species is further supported by the vibrational progression of $\Delta\nu$ = 1200 cm^{-1} observed for the 7-nm SiO_2-nanoparticles (upper trace in Figure 1). The $\Delta\nu$ = 1200 cm^{-1} progression is assigned as due to the bending vibration of interfacial water molecules ($\Delta\nu$ = 1595 cm^{-1} in gaseous H_2O) confined between SiO_2-nanoparticles (Figure 2), which comprise two Si–H's on the surface of one particle and one $Si-O\cdot$ on that of the other [44].

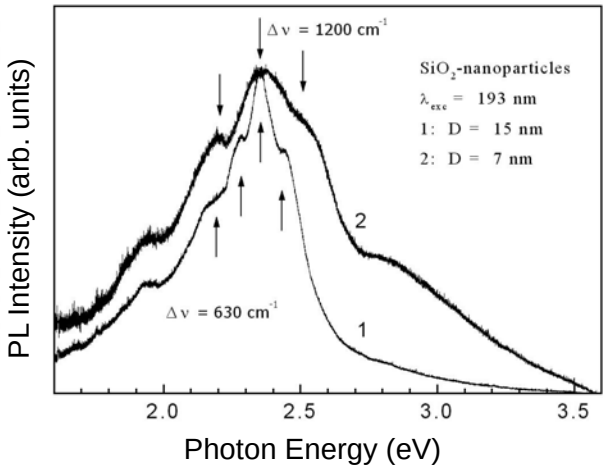

Figure 1. Normalized PL spectra of SiO_2-nanoparticles. Curve 1: particles of 15-nm diameter; Curve 2: particles of 7-nm diameter; λ_{exc} = 193 nm, I_L = 0.15 MW/cm^2

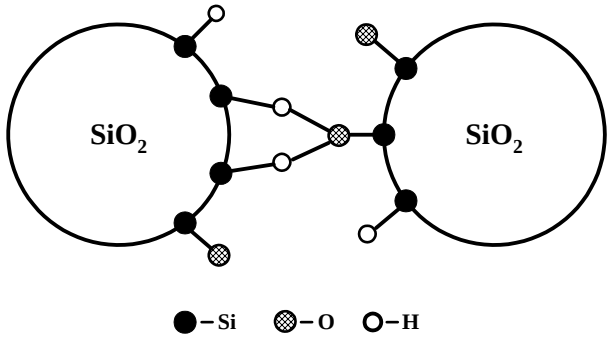

Figure 2. Interfacial water molecules confined between two SiO_2-nanoparticles

The blue band at ~2.8 eV observed in the 7-nm SiO_2-particles originates from the electron-hole recombination of self-trapped exciton (STE) as shown in Figure 3. The dynamical mechanism for the emission of the STE band in silica includes two processes. First, free excitons (FEs) in the conduction band of silica can be produced with two-photon excitation (hν = 12.8 eV) by an ArF laser. Some of the generated FEs could climb over or penetrate through a barrier to be trapped in a potential valley (namely, STE) where a defect of triplet electron-spin character is resulted from a bond-breaking of $Si-O$ (Figure 3). The excited triplet STE and the ground singlet state are responsible for the long lifetime (~1 ms in bulk silica) of the electron-hole recombination with emission energy of ~2.8 eV. This ~2.8 eV band is not pronounced for the 15-nm SiO_2-particles in Figure 1 with the CCD detection of 2-s accumulation, but can be much enhanced with a microsecond delay-gated measurement as will be shown (Figure 4) in the following section. The 2.8-eV band has been measured of a decay time-constant of ~5 μs at room temperature, and ~10 μs at 90 K for SiO_2-nanoparticles, which are much shorter than the ~1 ms of bulk silica [38,41]. The faster decay of the STE PL in SiO_2-nanoparticles is interpreted as an increase of the efficiency from FE to STE (Figure 3), accelerated by FE's gaining kinetic energy during the two-photon excitation (so called laser heating) [51,52].

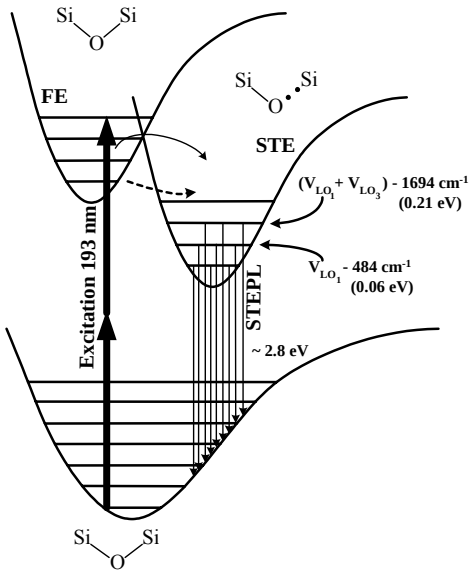

Figure 3. Schematic diagram in terms of the chemical bonding of $\equiv Si-O-Si\equiv$ clusters for the FEs and STEs in silica and their corresponding absorption and emission transitions. The solid and dashed arrows indicate crossing-over and tunneling-through the self-trapping barrier, respectively. Hot PL induced by phonon-assisted electronic transitions is also depicted

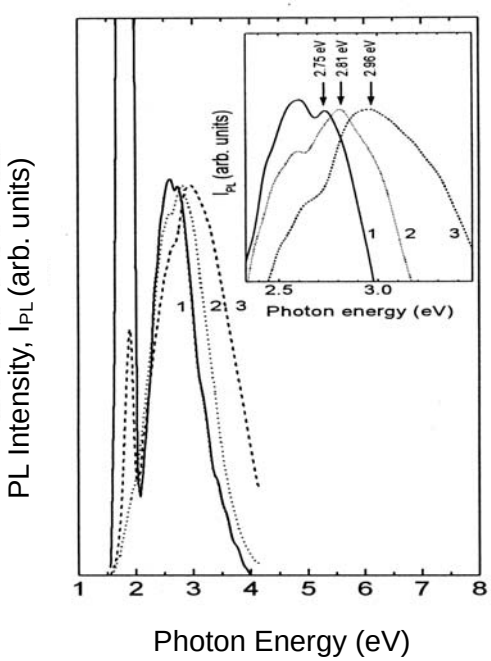

Figure 4. Normalized time delay-gated PL spectra for type-III fused silica (1), and SiO_2-nanoparticles with the sizes of 15 nm (2), and 7 nm (3) at 90 K and λ_{exc} = 193 nm (I_L = 1.15 MW/cm^2). An enlarged scale is shown in the inset. The spectra were detected with the following gate-delay/gate-width ratios in microseconds: 10/1 (1), 0/0.05 (2, 3).

3.2 Size Effect on the STE PL Shift

The time delay-gated PL spectra of 7-nm and 15-nm SiO_2-particles measured with ArF laser excitation (λ_{exc} = 193 nm) are shown in Figure 4. The PL spectra also compare the SiO_2-nanoparticles with type-III fused silica used as a corresponding bulk material. As discussed earlier, the PL spectra consist of red, green and blue bands. STE is responsible for the blue band at ~2.8 eV, and is our major interest here. Since the blue band is induced by a two-photon (TP) excitation, the band disappears gradually with decreasing laser light intensity, even though the green and red bands remain strong, indicating a decrease in the penetration efficiency through the STE barrier owing to the lack of kinetically energetic FEs (Figure 3) [51]. Note that the spectra presented in Figure 4 were optimized with appropriate gate-delay/gate-width parameters, with which the blue PL bands have their maximal intensities.

In Figure 4, the blue band for type-III fused silica is peaked at 2.75 eV with FWHM and a decay constant in good agreement with previous data [3]. However, the STE PL bands of the SiO_2-nanoparticles are blue-shifted relative to that of bulk silica (Figure 4), despite the green and red bands remain as the same as bulk silica. The enlarged blue-shifted STE PL bands are conveyed with arrows in the inset of Figure 4. While a shift of ~0.21 eV was observed for the 7-nm SiO_2-particles (peaked at 2.96 eV), ~0.06 eV is for the 15-nm particles (2.81 eV). It is noted that the resulting 2.81-eV and 2.96-eV bands are characterized by larger FWHMs (~0.8 and 1 eV, respectively) and smaller decay time-constants (τ~ 4 – 5 μs at 90 K).

3.3 Quantum Confinement Effect?

Can the blue-shift for smaller-sized SiO_2-nanoparticles observed in the STE PL spectra be explained by a widely used quantum confinement (QC) effect? It is generally accepted that QC theory has been developed for the Mott-Wannier type excitons of large Bohr-radius confined in nanoscale semiconductor materials [53,54]. Energy of excitons in semiconductors is represented as

$$E(D) = \frac{2\hbar^2\pi^2}{m^*_{e-h}D^2} \quad (1)$$

which is inversely proportional to the square of the material size (D). In our study, $E(D)$ has the minimum excitonic energy corresponding to that of

bulk material, and D is taken as the diameter of SiO_2-nanoparticles. In Eq. (1), the effective mass (m^*_{e-h}) of the exciton is taken as either

$$m^*_{e-h} = m^*_e + m^*_h \quad \text{or} \quad m^*_{e-h} = \frac{m^*_e m^*_h}{m^*_e + m^*_h} \quad (2)$$

corresponding to a weak or strong QC regime, respectively. m^*_e and m^*_h are effective electron and hole masses. From early experiment in silica glass, it is noted that $m^*_e = m^*_h \cong m$ [55], where $m = 9.11\times10^{-31}$ kg is the electron mass. Calculated from Eq. (2), $m^*_{e-h} = 18.22\times10^{-31}$ kg and 4.56×10^{-31} kg are obtained for weak and strong QC, respectively. Based on QC theory, we have fitted the observed blue-shifts of the STE PL bands in SiO_2-nanoparticles to Eq. (1). The fitting depicted as the curve 1 in Figure 5 renders $m^*_{e-h} = 1.31\times10^{-31}$ kg. Since the fitted m^*_{e-h} is smaller than that required for strong QC, one concludes that a strong QC is expected to occur in SiO_2-nanoparticles.

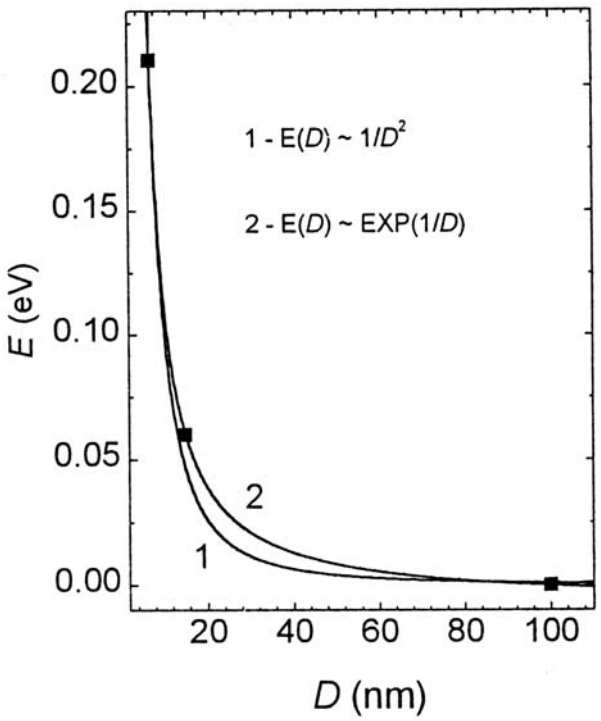

Figure 5. Observed blue-shifts of STE PL plotted against the primary sizes of SiO_2-nanoparticles (black squared points); the point marked for a 100-nm-sized particle corresponds to type-III fused silica. The fits to the data with the functions of $1/D^2$ and $exp(1/D)$ are drawn by the solid lines marked with 1 and 2, respectively

However, a weak or strong QC effect can alternatively be determined from the ratio of nanoparticle size (D) to the effective Bohr-radius (a^*_B) of the exciton in bulk material [54]. Two limiting cases, $a^*_B << D$ and $a^*_B >> D$, therefore correspond to the weak and strong QC regimes, respectively. Since the effective Bohr-radius (a^*_B) of STE in silica is estimated only ~0.5 nm [55], and the minimal diameter of nanoparticles in the present experiment is D = 7 nm, it is appropriate to apply a weak QC regime ($a^*_B << D$) to the SiO_2-nanoparticles in current study.

This contradiction reflects a limitation of applying QC theory developed for the Mott-Wannier excitons in semiconductors to describe the size effect on STE PL in nanoscaled wide band-gap silica material. In other words, the experimentally observed blue-shifts in SiO_2-nanoparticles are extraordinarily large compared to that expected from the QC theory.

3.4 Laser-Heating Model

In the optical excitation of SiO_2-based materials, it has been shown recently that the interaction of FEs with the nanoscale boundary can occur *either* as an energy transfer from FE to the surface of nano-objects followed by light emission, or as an elastic scattering without energy transfer [51,52]. The mean free path, L, for FE in bulk silica is much longer than the size of SiO_2-nanoparticles of the present study (for example, L ~ 500 nm in type-III fused silica) [1]. This indicates that FEs should suffer collisions severely with the boundary of confined space (Figure 6); that is, the collisions are so frequent that a FE is able to encounter many collisions in the applied laser-pulse duration (20 ns). In line of this reasoning, the collisional frequency tends to be higher with decreasing nanoparticle size.

In our experiment of SiO_2-nanoparticles, a TP excitation is necessary to generate FEs prior to the observation of STE PL. To activate the TP transition, high laser intensity (~10^6 W/cm^2) is usually required for the optical excitation [51], because the transition rate for a TP excitation is generally small [56]. Under this condition of strong laser irradiation, the FEs can additionally gain energy from the laser field, and be heated up to high temperature creating an electron-hole plasma. We have recently proposed that the laser heating of FEs results in an increase in the self-trapping rate and the formation of biexcitons relaxing into Frenkel defects [51-52].

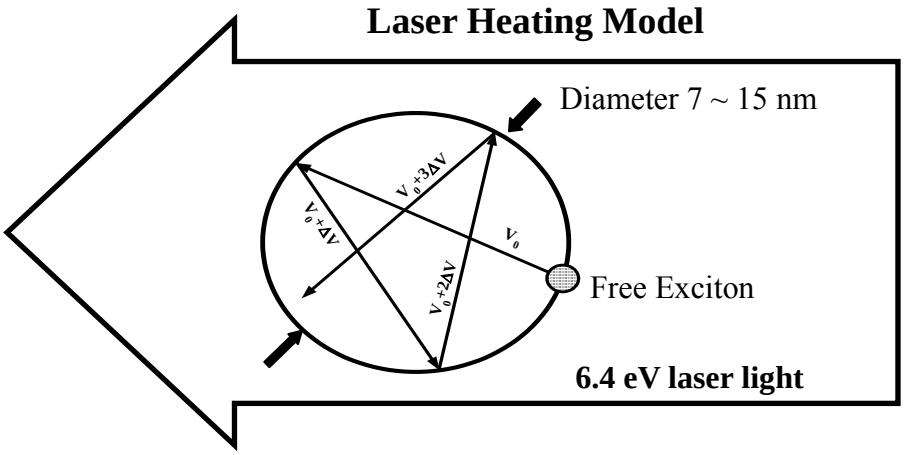

Figure 6. SiO_2-nanoparticles exposed to 6.4 eV laser radiation. The schematic illustrates the initially generated FE gaining kinetic energy (thus, velocity ΔV) in the subsequent collisions with the nanoscale boundary.

During the collisions with nanoscale boundary, the FE can gain additional energy from the laser field in a similar way as for electron-ion collisions in plasma [57-60]. Therefore, their maximal kinetic energy $E_{e\text{-}h}$ can be expressed as [59,60]

$$E_{e\text{-}h} = E_{ini} + E_{max} \tag{3}$$

where E_{ini} is the initial energy of FEs after their production, and E_{max} is the greatest possible energy of FEs gained within the laser heating process,

$$E_{max} = \sum_{n=1}^{\kappa} \Delta E^{(n)} = \kappa \Delta E^{(n)} \tag{4}$$

where κ is the maximal number of collisions within the laser pulse duration of τ_L , and $\Delta E^{(n)}$ denotes the energy increment due to a single collision, which corresponds to an increment of the velocity (ΔV) of FE (Figure 6). The energy increment $\Delta E^{(n)}$ of FE can be found similar to that of electron in ionized plasma under laser irradiation [57-60].

Accordingly, the energy rate equation for an electron in ionized plasma at the presence of an intense laser field of amplitude E_0 is expressed as [57-60]

$$\frac{dE}{dt} = \frac{e^2 E_0^2 \nu}{2m(\omega^2 + \nu^2)} - \frac{2Em\nu}{M} \tag{5}$$

where the first term describes the energy gain and the second one corresponds to the energy loss due to collisions with nanoscale boundary (Figure 6). In Eq. (5), *e* and *m* represent electron charge and mass; *M* is the surface atom, and ω and ν denote the frequencies of laser field and collisions, respectively. Eq. (5) is just a Bernoulli's differential equation. The solution, with the initial condition of $E = 0$ at $t = 0$, under a direct integration within the laser pulse duration of τ_L gives

$$E = \frac{Me^2E_0^2}{4m^2(\omega^2+\nu^2)}\left[1-\exp(\frac{2m\nu\tau_L}{M})\right] \approx \frac{e^2E_0^2\nu\tau_L}{2m(\omega^2+\nu^2)} = \frac{\lambda^2 r_e I_L \nu\tau_L}{\pi c(1+\nu^2/\omega^2)} \approx \frac{\lambda^2 r_e I_L \nu\tau_L}{\pi c} \tag{6}$$

where it has been reasonably assumed that $M >> m$ and $\omega >> \nu$, and also taken into account that the laser intensity is $I_L = (c/8\pi)E_0^2$; $\lambda = 2\pi c/\omega$ is the laser wavelength; $r_e = e^2/mc^2$ is the classical electron radius, and *c* denotes the velocity of light in vacuum. It can be easily seen from Eq. (6) that the energy gained by the electron depends linearly on the laser intensity indicating a single-photon inverse Bremsstrahlung process. After some mathematical procedures, with which the details can be found in Ref. 60, the kinetic energy of free exciton finally gives

$$E_{e-h} = \frac{2\lambda^2 r_p I_L^{eff}}{\pi c_m} exp\left[2\lambda\left(\frac{2\tau_L}{D}-\frac{1}{V_0}\right)\left(\frac{r_p I_L^{eff}}{m_{e-h}^* \pi c_m}\right)^{1/2} - 0.577\right] \tag{7}$$

where V_0 is the initial velocity of FE; $r_p = e^2/\varepsilon m_e^* c_m^2$ is the corresponding polaron radius, ε and c_m are the dielectric constant and the velocity of light in a medium, respectively; $I_L^{eff} = (c_m/8\pi)[E_0 + (\varepsilon_\infty - 1)E_0/3]^2$ is the effective laser intensity [61]. It is proved from Eq. (7) that at the fixed parameters of the laser excitation (λ, I_L, τ_L) and the material used (V_0, m_{e-h}^*, c_m, r_p), the energy gained by FEs through laser heating process increases with decreasing nanoparticle diameter as a function of *exp(1/D)*. Also, the efficiency of laser heating for FEs should be much higher with increasing wavelength, intensity, and

pulse duration of the applied laser light.

3.5 Phonon-Assisted PL

The fit of the blue-shifts observed in the STE PL of SiO_2-nanoparticles to *exp(1/D)* is shown as the curve 2 in Figure 5. From the comparison between QC theory (curve 1) and laser-heating model (curve 2), it is clear that the latter is more appropriate to account for the observations.

As mentioned earlier, the self-trapping of FEs is caused by a localization of the FEs in lattice resulting in a reduction of the excitonic energy (Figure 3) [61]. To reach the STE potential valley, there exists a barrier for FEs to climb over or penetrate through (Figure 3) [61]. From previous study, we have shown that the energetic activation of FEs by laser-excitation to cross over the barrier enhances the efficiency of self-trapping [51]. Therefore, the penetration efficiency of FE through the STE barrier increases with the FE temperature (kinetic energy), and reaches its maximum when the FE energy is enough to overcome the barrier. It is noted that hot STEs can occur after the FEs pass the STE barrier, and the thermalization of STEs is dominated by the excitation of lattice phonons (i.e. balance between cooling the STEs and heating the SiO_2-nanoparticle system). However, if an equilibrium is achieved between the electron-hole and lattice-phonon subsystems, the STE is able to either emit or absorb phonons. As a consequence, hot PL induced by phonon-assisted electronic transitions can occur at this equilibrium condition.

There exist three types of LO (longitudinal-optical) and TO (transverse-optical) phonon modes in SiO_2-based materials [39], including three different local vibrational motions of the oxygen atoms with respect to the silicons: the rocking, bending, and asymmetrical stretching motions, respectively. The corresponding frequencies are: TO_1 = 424 cm^{-1} (0.053 eV), LO_1 = 471 cm^{-1} (0.058 eV), TO_2 = 791 cm^{-1} (0.098 eV), LO_2 = 1005 cm^{-1} (0.125 eV), TO_3 = 1086 cm^{-1} (0.135 eV), LO_3 = 1206 cm^{-1} (0.150 eV). Take a close look at the blue-shifts of the STE PL in our study, 0.06 eV and 0.21 eV are observed for the 15-nm and 7-nm SiO_2-nanoparticles, respectively. The STE PL blue shift of 0.06 eV for 15-nm particles can be attributed to the activation of LO_1 phonon-assisted transitions (Figure 3). The more energetic phonons of 0.21 eV found in 7-nm particles is in full agreement with the theoretical prediction that kinetic activation of FEs is more pronounced in the particles of smaller size. Accordingly, the emission band at 2.96 eV (0.21 eV shift) in 7-nm SiO_2-particles is assisted by a combined phonon modes of $LO_1 + LO_3$ (0.058 + 0.15 = 0.208 eV) (Figure 3). These phonon- assisted PL bands therefore nicely account for the blue-shifts of the STE PL observed in the SiO_2-nanoparticles.

4. Conclusions

The observed PL spectra of SiO_2- nanoparticles consist of three major contributions located in the red (~1.9 eV, NBO), green (~2.35 eV, hydrogen-related species), and blue (~2.8 eV, STE) spectral ranges. General QC theory used for semiconductors is not appropriate to explain the size effect on PL shift in a wide band-gap material, such as silica. We have developed a laser-heating model to illuminate the blue-shift of STE PL in smaller-sized SiO_2-nanoparticles, which is actually resulted from phonon-assisted PL due to the thermalization of the SiO_2-nanoparticle system during laser irradiation.

Acknowledgments

I wish to thank Dr. Yuri D. Glinka for his tremendous contribution to the work presented in this article, and to express my appreciation of the collaboration with Professor S. H. Lin in various research subjects over the past years. This work is supported by National Science Council of R.O.C. (NSC-90-2113-M-001-037).

References

[1] Trukhin, A. N. *J. Non-Cryst. Solids* **1992**, *149*, 32.
[2] Arai, K.; Imai, H.; Hosono, H.; Abe, Y.; Imagawa, H. *Appl. Phys. Lett.* **1988**, *53*, 1891.
[3] Itoh, C.; Tanimura, K.; Itoh, N.; Itoh, M. *Phys. Rev. B* **1989**, *39*, 11183.
[4] Awazu, K.; Kawazoe, H. *J. Appl. Phys.* **1990**, *68*, 3584.
[5] Nishikawa, H.; Nakamura, R.; Tohmon, R.; Ohki, Y.; Sakurai, Y.; Nagasawa, K.; Hama, Y. *Phys. Rev. B* **1990**, *41*, 7828.
[6] Itoh, C.; Suzuki, T.; Itoh, N. *Phys. Rev. B* **1990**, *41,* 3794.
[7] Shluger, A.; Stefanovich, E. *Phys. Rev. B* **1990**, *42*, 9664.
[8] Imai, H.; Arai, K.; Hosono, H.; Abe, Y.; Arai, T.; Imagawa, H. *Phys. Rev. B* **1991**, *44*, 4812.
[9] Tsai, T. E.; Griscom, D. L. *Phys. Rev. Lett.* **1991**, *67*, 2517.
[10] Griscom, D. L. *J. Ceram. Soc. Jpn.* **1991,** *99*, 923.
[11] Joosen, W.; Guizard, S.; Martin, P.; Petite, G.; Agostini, P.; Dos Santos, A.; Grillon, G.; Hulin, D.; Migus, A.; Antonetti, A. *Appl. Phys. Lett.* **1992**, *61*, 2260.
[12] Kuzuu, N.; Matsumoto, Y.; Murahara, M.

Phys. Rev. B **1993**, *48*, 6952.
[13] Skuja, L. *J. Non-Cryst. Solids* **1994**, *179*, 51.
[14] Wilson, M.; Madden, P. A.; Hemmati, M.; Angell, C. A. *Phys. Rev. Lett.* **1996**, *77*, 4023.
[15] Skuja, L.; Guttler, B. *Phys. Rev. Lett.* **1996**, *77*, 2093.
[16] Skuja, L.; Tanimura, K.; Itoh, N. *J. Appl. Phys.* **1996**, *80*, 3518.
[17] Pasquarello, A.; Car, R. *Phys. Rev. Lett.* **1997**, *79*, 1766.
[18] Kuzuu, N.; Taga, T.; Kamisugi, N. *J. Appl. Phys.* **1997**, 81, 8011.
[19] Guillot, B.; Guissani, Y. *Phys. Rev. Lett.* **1997**, *78*, 2401.
[20] Boero, M.; Pasquarello, A.; Sarnthein, J.; Car, R. *Phys. Rev. Lett.* **1997,** *78*, 887.
[21] Nishikawa, N.; Miyake, Y.; Watanabe, E.; Ito, D.; Seol, K. S.; Ohki, Y.; Ishii, K.; Sakurai, Y.; Nagasawa, K. *J. Non-Cryst. Solids* **1997,** *222*, 221.
[22] Pacchioni, G.; Ierano, G.; Marquez, A. *Phys. Rev. Lett.* **1998**, *81*, 377.
[23] Skuja, L. *J. Non-Cryst. Solids* **1998**, *239*, 16.
[24] Skuja, L.; Guttler, B.; Schiel, D.; Silin, A. R. *Phys. Rev. B* **1998**, *58*, 14296.
[25] Stevens Kalceff, M. A. *Phys. Rev. B* **1998**, *57*, 5674.
[26] Pacchioni, G.; Vitiello, M. *Phys. Rev. B* **1998**, *58*, 7745.
[27] Hosono, H.; Kawazoe, H.; Matsunami, N. *Phys. Rev. Lett.* **1998**, *80*, 317.
[28] Griscom, D. L.; Mizuguchi, M. *J. Non-Cryst. Solids* **1998**, *239*, 66.
[29] Griscom, D. L. *in Proceedings of the Thirty-Third Frequency Control Symposium;* Electronics Industries Assn., Washington, D. C., U.S.A., **1980**; pp 98.
[30] Conley, J. F.; Lenaham, P. M. *Appl. Phys. Lett.* **1993**, *62*, 40.
[31] Hess, K.; Tuttle,B. ; Register, F. ; Ferry, D. K. *Appl. Phys. Lett.* **1999**, *75*, 3147.
[32] Tsybeskov, L.; Grom, G. F.; Fauchet, P. M.; McCaffrey, J. P.; Baribeau, J.-M.; Sproule, G. I.; Lockwood, D. J. *Appl. Phys. Lett.* **1999**, *75*, 2265.
[33] Grom, G. F.; Lockwood, D. J.; McCaffrey, J. P.; Labbe, H. J.; Fauchet, P. M.; White, B.; Diener, J.; Kovalev, D.; Koch, F.; Tsybeskov, L. *Nature* **2000**, *407*, 358.
[34] Pavesi, L.; Dal Negro, L.; Mazzoleni, C.; Franzo, G.; Priolo, F. *Nature* **2000**, *408*, 440.
[35] Lucovsky, G.; Yang, J.; Chao, S. S.; Tyler, J. E.; Czubatyj, W. *Phys. Rev. B* **1983**, *28*, 3225.
[36] Glinka, Yu. D.; Naumenko, S. N.; Degoda, V. Ya. *J.Non-Cryst. Solids* **1993**, *152*, 219.
[37] El-Shall, M. S.; Li, S.; Turkki, T.; Graiver, D.; Pernisz, U. C.; Baraton, M. I. *J. Phys. Chem. B* **1995**, *99*, 17805.
[38] Seol, K. S.; Ohki, Y.; Nishikawa, H.; Takiyama, M.; Hama, Y. *J. Appl. Phys.* **1996**, *80*, 6444.
[39] Glinka, Yu. D.; Jaroniec, M. *J. Appl. Phys.* **1997**, *82*, 3499.
[40] Glinka, Yu. D. *JETP* (Eng. Transl.) **1997**, *84*, 957.
[41] Goldberg, M.; Fitting, H.-J.; Trukhin, A. *J. Non-Cryst. Solids* **1997**, *220*, 69.
[42] Trukhin, A. N.; Goldberg, M.; Jansons, J.; Fitting, H.-J.; Tale, I. A. *J. Non-Cryst. Solids* **1998**, *223*, 114.
[43] Prokes, S. M.; Carlos, W. E.; Veprek, S.; Ossadnic, Ch. *Phys. Rev. B* **1998**, *58*, 15632.
[44] Glinka, Yu. D.; Lin, S. H.; Chen, Y.-T. *Appl. Phys. Lett.* **1999**, *75*, 778.
[45] Wilson, W. L.; Szajowski, P. F.; Brus, L.E. *Science* **1993**, *262*, 1242.
[46] Brus, L. E.; Szajowski, P. F.; Wilson, W. L.; Harris, T. D.; Schuppler, S.;Citrin, P. H. *J. Am. Chem. Soc.* **1995**, *117*, 2915.
[47] Canham, L. T. *Appl. Phys. Lett.* **1990**, *57*, 1046.
[48] Cullis, A. G.; Canham, L. T.; Calcott, P. D. J. *J. Appl. Phys.* **1997**, *82*, 909.
[49] Holmes, J. D.; Johnston, K. P.; Doty, R. C.; Korgel, B. A. *Science* **2000**, *287*, 1471.
[50] Wolkin, M. V.; Jorne, J.; Fauchet, P. M.; Allan, G.; Delerue, C. *Phys. Rev. Lett.* **1999**, *82*, 197.
[51] Glinka, Yu. D.; Lin, S. H.; Chen, Y.-T. *Phys. Rev. B* **2000**, *62*, 4733.
[52] Glinka, Yu. D.; Lin, S. H.; Hwang, L. P.; Chen, Y.-T. *J. Phys. Chem. B* **2000**, *104*, 8652.
[53] Efros Al. L.; Efros, A. L. *Fiz. Tekh. Poluprovodn.* **1982,** *16*, 1209.
[54] Brus, L. E. *J. Chem. Phys*. **1983**, *79*, 5566.
[55] Godmanis, I. T.; Trukhin, A. T.; Hubner, K. *Phys. Status Solidi B* **1983**, *116*, 279.
[56] Shen, Y. R. *The Principles of Nonlinear Optics;* Wiley, New York, U.S.A., **1984**.
[57] Bunkin, F. B.; Kazakov, A. E.; Fedorov, M. V. *Sov. Phys. Usp.* **1973**, *15*, 416.
[58] Kroll N. M.; Watson, K. M. *Phys. Rev. A* **1973**, *8*, 804.
[59] Glinka Yu. D.; Jaroniec, M. *Phys. Rev. A* **1997**, *56*, 3056.
[60] Glinka, Yu. D.; Hwang, L. P.; Lin, S. H.; Chen,Y.-T.; Tolk, N. H. *Phys. Rev. B* **2001**, *64*, 085421.
[61] Rashba, E. I. *Excitons*; Rashba, E. I. and Sturge, M. D., Ed.; Elsevier, Amsterdam, **1987**; pp 273.

Manuscript Received: Apr. 15, 2002
and Accepted: May 17, 2002